Spectral compression in a comb-like distributed fiber and its application in 7-bit all-optical quantization

Ying Chen
Zhiyao Zhang
Xiaojun Zhou
Xiangning Chen
Yong Liu

Spectral compression in a comb-like distributed fiber and its application in 7-bit all-optical quantization

Ying Chen,[a,b,]* Zhiyao Zhang,[b] Xiaojun Zhou,[b] Xiangning Chen,[a] and Yong Liu[b]
[a]Academy of Equipment, No. 172, Mailbox 3380, Beijing 101416, China
[b]University of Electronic Science and Technology of China, School of Optoelectronic Information, State Key Laboratory of Electronic Thin Films and Integrated Devices, No. 4, Section 2, North Jianshe Road, District of Chenghua, Chengdu 610054, China

Abstract. Subpicosecond pulse spectral compression without the limitation of the adiabatic soliton transform status in a comb-like distributed fiber (CDF) is proposed and numerically demonstrated. The principle of spectral compression in a single concatenation of single-mode fiber and high nonlinear fiber is theoretically analyzed and numerically proved. A three-stage CDF is designed and simulated following the principle. The simulation results show that an overall spectral compression ratio of 56.23 is obtained. The designed three-stage CDF is used in an all-optical analog-to-digital system to improve the quantization resolution to 7.1 bit. © *The Authors. Published by SPIE under a Creative Commons Attribution 3.0 Unported License. Distribution or reproduction of this work in whole or in part requires full attribution of the original publication, including its DOI.* [DOI: 10.1117/1.OE.53.12.126106]

1 Introduction

Since comb-like dispersion profiled fiber (CDPF) was first investigated in Ref. 1 for the soliton pulse train generation, a series of research has been implemented to analyze this cascaded structure.[2–9] CDPF is generally composed of a number of alternating lengths of high and low dispersion fibers [i.e., single mode fibers (SMFs) and dispersion shifting fibers (DSFs)] in which the dispersion effect and nonlinearity effect are spatially separated.[2] However, since the calculation and optimization for the dispersion, nonlinearity, and length of each fiber in CDPF are complex, a comb-like profiled fiber (CPF) was introduced to simplify the interconnected structure by using only two types of fibers, SMF and high nonlinearity fiber (HNLF).[3] CPF is widely used in the fields of pedestal-free adiabatic soliton pulse compression, high-repetition rate short optical soliton pulse train generation, wavelength-tunable femtosecond pulse source and, so on.[2–9] Recently, it has been found that a new application of CPF has the advantage of improving the resolution of an all-optical analog-to-digital conversion system.[10–13] In Ref. 10, the CPF composed of 19 segments of SMF and DSF is employed to realize a DSF to implement the adiabatic soliton spectral compression, giving a spectral compression ratio of up to 19.8 to 25.9. However, to the best of our knowledge, spectral compression without the limitation of adiabatic soliton status in a dispersion comb-like profiled fiber has never been studied and only a few works have demonstrated the wide wavelength-tunable abilities of spectral compression in CPF.

In this paper, the principle of spectral compression in a comb-like distributed fiber (CDF) based on a novel chirp-compensation method is analyzed by a strict theoretical derivation. The theoretical analysis shows that complete chirp compensation between the self-phase modulation effect

(SPM) and group velocity dispersion (GVD) is the key to the design of the CDF. The three-stage CDF consisting of three concatenations of SMF and HNLF is carefully designed by solving the generalized nonlinear Schrödinger equation in the numerical simulation. The simulation results show that the spectral width is compressed from 11.8 to 0.21 nm, obtaining a spectral compression ratio up to 56.2. Using this technique, after shifting the soliton spectrum is sharply compressed and the all-optical quantization resolution of the all-optical analog-to-digital conversion (ADC) system is successfully improved towards 7.1-bit.

2 Principle

2.1 Spectral Compression in a Single Concatenation of Single-Mode Fiber + High Nonlinearity Fiber

The spectral compression in a single concatenation of SMF +HNLF is well understood as a process of chirp compensation.[14–16] The pulse is highly negatively chirped by the GVD effect by passing through the SMF (e.g., red line in Fig. 1). Then, chirp induced by the SPM in the HNLF has a nearly linear positive slope around the center of the pulse (e.g., blue line in Fig. 1), which can compensate the GVD-induced negative chirp. The central part of the spectrum is compressed since both the long and short wavelengths are shifted toward the central wavelength. This process is called the nonlinear chirp compensation in the paper.

Moreover, the compensation extent of two different chirps around the pulse center determines the spectral compression quality. Figure 2(a) shows the spectral compression under the condition of three cases of chirp compensations: insufficient compensation, complete compensation, and overcompensation. The respective compensated chirps are presented in Fig. 3(b). It is obvious that the spectral compression is not finished when the compensation is insufficient, leading to a poor spectral compression ratio (SCR), which is defined as the ratio of the input to the output spectral width (FWHM).

---

*Address all correspondence to: Ying Chen, E-mail: kensub@126.com
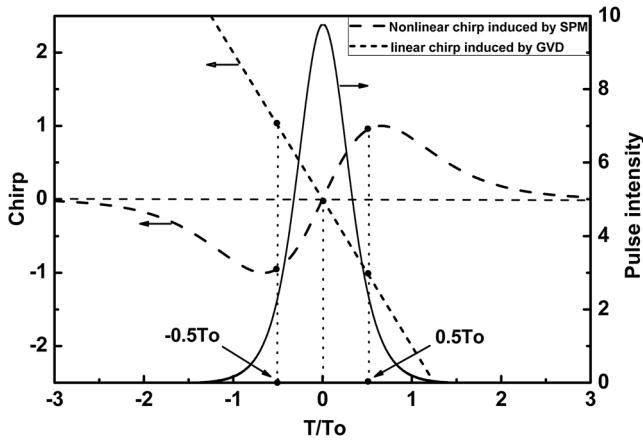
Fig. 1 The compensation of chirp induced by group velocity dispersion (GVD) and self-phase modulation effect (SPM) around the central pulse in a concatenation of single-mode fiber (SMF) and high non-linearity fiber (HNLF).

A higher spectral compression ratio can be obtained under the condition of overcompensation, but the pedestal and the side-lobe components are drastically raised, significantly degrading the compressed spectrum quality. Hence, when the absolute value of two chirps is equal but the signs are opposite, the dispersion-induced chirp is totally cancelled by the SPM-induced chirp around the center wavelength, resulting in a high enough spectral compression ratio and suppressed side-lobe components. The conclusion can be drawn that an excellent trade-off between the spectral compression ratio and spectral compression quality has been made when the chirp is precisely compensated near the central wavelength.

2.2 Theoretic Derivation of Comb-Like Distributed Fiber Based on Nonlinear Chirp Compensation Model

CDF is composed of several concatenations of SMF and HNLF such as the three-stage CDF shown in Fig. 3. Each concatenation of SMF and HNLF should satisfy the condition that the GVD-induced chirp in SMF is completely compensated by the SPM-induced chirp in HNLF, so that the

central part of the pulse is chirp-free and can be prechirped in the next SMF. In general, the process of spectral compression in CDF is a repetition of the complete chirp compensation around the central wavelength. As the other parameters are decided when the fibers are chosen, the lengths of SMF and HNLF are the only factor which could determine the extent of chirp compensation. Therefore, how to calculate the fibers' length is the key to the design of the whole system based on the chirp compensation model. In order to prove the theoretical analysis, a strict derivation to calculate the fibers' length is provided next.

A chirp-free Gaussian pulse, with a central wavelength of 1550 nm, a duration of T_0 (FWHM), and a peak power of P_0 ($P_0 = E_0^2$), is used as an the input of the system. The SMF has a dispersion coefficient of β_2 while the nonlinear coefficient of HNLF is a constant of λ. The lengths of the first concatenation of SMF and HNLF (named SMF1 and HNLF1) are S_1 and H_1, respectively. The input pulse can be expressed in the time and frequency domains.[17]

$$\begin{cases} E_0(T) = E_0 \exp\left(-\dfrac{T^2}{2T_0^2}\right) = \sqrt{P_0} \exp\left(-\dfrac{T^2}{2T_0^2}\right) \\ E_0(\omega) = E_0\sqrt{2\pi T_0^2} \exp\left(-\dfrac{T_0^2\omega^2}{2}\right) = \sqrt{2\pi P_0 T_0^2} \exp\left(-\dfrac{T_0^2\omega^2}{2}\right) \end{cases}.$$
$$(1)$$

Only considering the group velocity dispersion effect in the SMF, the distribution in the frequency domain $E_1(\omega)$ after pulse transmission in SMF1 is

$$\begin{aligned} E_1(\omega) &= E_0(\omega)\,\exp\left(\frac{j}{2}\beta_2 S_1 \omega^2\right) \\ &= E_0\sqrt{2\pi T_0^2}\exp\left(-\frac{T_0^2 - j\beta_2 S_1}{2}\omega^2\right). \end{aligned}$$
$$(2)$$

Using the Fourier transform pair of $e^{-(t/\tau)^2} \overset{\text{FFT}}{\underset{\text{iFFT}}{\rightleftarrows}} \sqrt{\pi}\,\tau e^{-(\omega\tau/2)^2}$, assuming $\tau^2 = 2(T_0^2 - j\beta_2 S_1)$, we can obtain the respective distribution in the time domain $E_1(T)$.
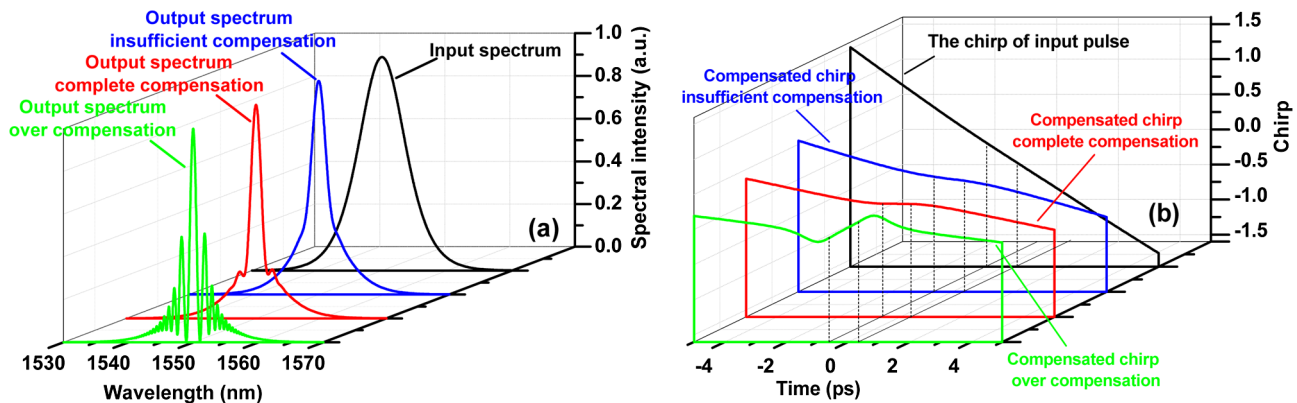

Fig. 2 (a) Spectral compression in single concatenation of SMF and HNLF under three different chirp-compensation conditions: insufficient compensation (blue line); complete compensation (red line), and over compensation (green line) near the central wavelength. (b) Input pulse chirp and three different compensated chirps in single concatenation of SMF and HNLF.
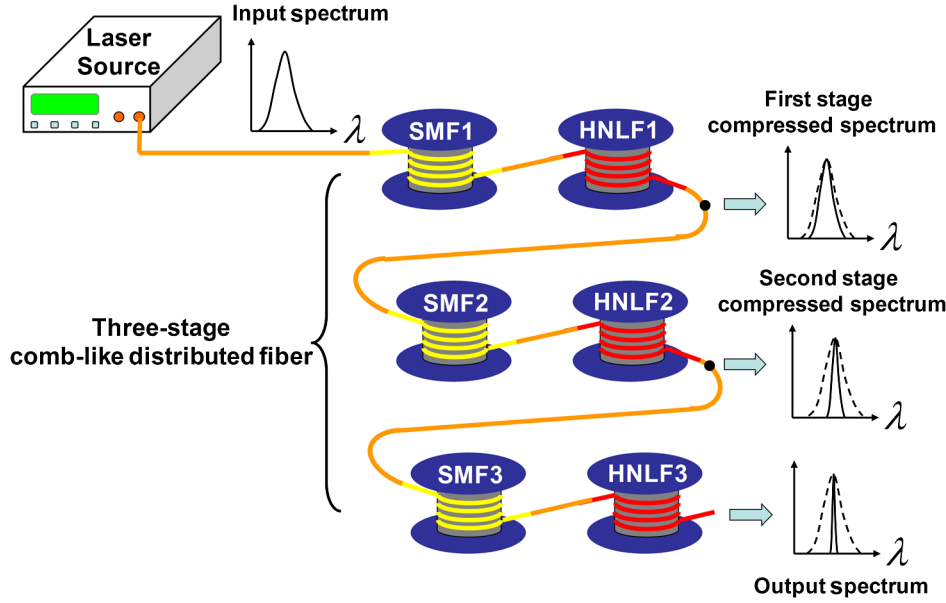
Fig. 3 Schematic diagram of three-level nonlinear comb-like distributed fibers (CDFs).

$$E_1(T) = \frac{E_0 T_0}{\sqrt{T_0^2 - j\beta_2 S_1}} \exp\left[-\frac{T^2}{2(T_0^2 - j\beta_2 S_1)}\right]. \tag{3}$$

Simplifying Eq. (3):

$$E_1(T) = \frac{E_0 T_0}{(T_0^4 + \beta_2^2 S_1^2)^{\frac{1}{4}}} \exp\left[-\frac{T^2 T_0^2}{2(T_0^4 + \beta_2^2 S_1^2)}\right]$$
$$\times \exp\left\{j\left[\frac{1}{2}\arctan\frac{\beta_2 S_1}{T_0^2} - \frac{\beta_2 S_1 T^2}{2(T_0^4 + \beta_2^2 S_1^2)}\right]\right\}. \tag{4}$$

From Eq. (4), we can gain the linear phase shift $\phi_{\mathrm{GVD}-S_1}$ in the SMF1:

$$\phi_{\mathrm{GVD}-S_1} = -\frac{\beta_2 S_1 T^2}{2(T_0^4 + \beta_2^2 S_1^2)} + \frac{1}{2}\arctan\frac{\beta_2 S_1}{T_0^2}. \tag{5}$$

Then, the chirp induced by GVD ($\delta\omega_{\mathrm{GVD}-S_1}$) in the SMF1 can be calculated by taking the derivative with respect to $\phi_{\mathrm{GVD}-S_1}$.

$$\delta\omega_{\mathrm{GVD}-S_1} = -\frac{\mathrm{d}\phi_{\mathrm{GVD}-S_1}}{\mathrm{d}T} = -\frac{\beta_2 S_1}{T_0^4 + \beta_2^2 S_1^2} T. \tag{6}$$

After the transmission in the SMF1, the pulse E_1 keeps transmitting in the HNLF1. Similarly, only considering the self-phase shifting effect in the HNLF1, the nonlinear phase shifting in the HNLF1 can be calculated as follows:[17]

$$\phi_{\mathrm{SPM}-H_1} = |E_1(T)|^2 \gamma H_1$$
$$= \frac{E_0^2 \gamma H_1 T_0^2}{(T_0^4 + \beta_2^2 S_1^2)^{\frac{1}{2}}} \exp\left(-\frac{T^2 T_0^2}{T_0^4 + \beta_2^2 S_1^2}\right). \tag{7}$$

The chirp induced by SPM ($\delta\omega_{\mathrm{SPM}-H_1}$) in the SMF1 can be calculated by taking the derivative with respect to $\phi_{\mathrm{SPM}-H_1}$.

$$\delta\omega_{\mathrm{SPM}-H_1} = -\frac{\mathrm{d}\phi_{\mathrm{SPM}-H_1}}{\mathrm{d}T}$$
$$= \frac{2E_0^2 \gamma H_1 T_0^4}{(T_0^4 + \beta_2^2 S_1^2)^{\frac{3}{2}}} \exp\left(-\frac{T^2}{T_0^2 + \frac{\beta_2^2 S_1^2}{T_0^2}}\right) T. \tag{8}$$

In order to simplify Eq. (8), the nonlinear part of $\exp[-T^2/T_0^2 + (\beta_2^2 S_1^2/T_0^2)]$ can be neglected as the constant of 1. The reason is described as follows:

First, the magnitude order of a typical β_2 is 10^{-27} (s²/m), otherwise a typical pulse duration has a number scale of 10^{-15} (s). Therefore, the part of $\beta_2^2 S_1^2/T_0^2$ is approximate to the value of zero. Besides, the chirp compensation would happen around the central wavelength of the pulse, e.g., $-0.3T_0 < T < 0.3T$. Assuming that $T = 0.3T_0$, the value of $\exp(-T^2/T_0^2)$ is equal to 0.9139, which is close to 1. Therefore, we can make an approximation that the nonlinear part of $\exp[-T^2/T_0^2 + (\beta_2^2 S_1^2/T_0^2)]$ can be neglected as the constant of 1. Then,

$$\delta\omega_{\mathrm{SPM}-H_1} = \frac{2E_0^2 \gamma H_1 T_0^4}{(T_0^4 + \beta_2^2 S_1^2)^{\frac{3}{2}}} \exp\left(-\frac{T^2}{T_0^2 + \frac{\beta_2^2 S_1^2}{T_0^2}}\right) T$$
$$\approx \frac{2E_0^2 \gamma H_1 T_0^4}{(T_0^4 + \beta_2^2 S_1^2)^{\frac{3}{2}}} T. \tag{9}$$

The key of the chirp compensation model is the precisely complete chirp compensation between the GVD-induced and SPM-induced chirps around the central wavelength of the pulse. Therefore,

$$\delta\omega_{\mathrm{GVD}-S_1} = \delta\omega_{\mathrm{SPM}-H_1}, \tag{10}$$

$$-\frac{\beta_2 S_1}{T_0^4 + \beta_2^2 S_1^2} T = E_0^2 \gamma H_1 \frac{2T_0^4}{(T_0^4 + \beta_2^2 S_1^2)^{\frac{3}{2}}} T. \tag{11}$$

From Eq. (11), we can gain the relationship between the lengths of the SMF1 and HNLF1 as follows:

$$H_1 = -\frac{\beta_2 S_1 \sqrt{T_0^4 + \beta_2^2 S_1^2}}{2\gamma P_0 T_0^4}. \tag{12}$$

It can be concluded from Eq. (11) that the length of HNLF1 is only determined by the length of SMF1 when the fibers are selected, which just simplifies the design of the CDF.

Similarly, the length of the next concatenation of SMF and HNLF $(S_2, H_2, S_3, H_3, \ldots)$ can be precisely calculated following the derivation above and is shown as follows:

$$H_2 = -\frac{S_2 \beta_2 \sqrt{(T_0^4 + \beta_2^2 S_1^2)^2 + T_0^4 \beta_2^2 S_2^2}}{2E_0^2 T_0^2 \gamma (T_0^4 + \beta_2^2 S_1^2)^{\frac{3}{2}}}, \tag{13}$$

$$H_3 = \frac{[\beta_2 S_3 T_0^2 (T_0^4 + \beta_2^2 S_1^2)]}{2E_0^2 T_0^2 \gamma [(T_0^4 + \beta_2^2 S_1^2)^2 + T_0^4 \beta_2^2 S_2^2]^{3/2}}$$

$$\left\{ \frac{[(T_0^4 + \beta_2^2 S_1^2)^2 + T_0^4 \beta_2^2 S_2^2]^2 + [\beta_2 S_3 T_0^2 (T_0^4 + \beta_2^2 S_1^2)]^2}{T_0^4 + \beta_2^2 S_1^2} \right\}^{\frac{1}{2}}. \tag{14}$$

Equations (12) to (14) reveal the relationship between the length of HNLF, SMF, and the parameters of two types of fibers based on the complete nonlinear chirp compensation in the CDF. The result of derivation is used in the CDF design in the next section.

3 Design and Simulation of the Comb-Like Distributed Fiber

To prove the analytical derivation above, a three-stage CDF is designed which is strictly calculated following the derivation. The calculation results of the length of each SMF and HNLF are shown in Fig. 4. The numerical simulation is simultaneously carried out for certification. The pulse propagation in the CDF is described by the nonlinear Schrödinger equation:

$$\frac{\partial A}{\partial z} + \frac{i}{2}\beta_2 \frac{\partial^2 A}{\partial T^2} - \frac{1}{6}\beta_3 \frac{\partial^3 A}{\partial T^3} = -\frac{\alpha}{2}A + i\gamma|A|^2 A, \tag{15}$$

where β_2 and β_3 are second- and third-order dispersions, respectively, α is the loss coefficient, and γ is the nonlinear coefficient. Equation (15) is solved by using the split-step

Table 1 Second-order dispersion β_2, third-order dispersion β_3, the nonlinear coefficient γ, and the loss coefficient α of the single-mode fiber (SMF) and high nonlinearity fiber (HNLF).

	β_2 (ps²/km)	β_3 (ps³/km)	γ (W⁻¹km⁻¹)	α (dB/km)
SMF	−19.37	0.1879	2	0.2
HNLF	−3.8237	0.01444	27	0.22

Fourier method.[17] Figure 4 shows the design of a three-stage CDF composed of SMF and HNLF, in which each fiber length is labeled. The parameters of SMF and HNLF are listed in Table 1. In the simulation, a chirp-free Gaussian pulse, with a central wavelength of 1550 nm, a duration of 300 fs (FWHM), and a peak power of 6.7 W, is used as the input of the CDF.

The simulation results are shown in Figs. 5–7. In the first concatenation, the input spectrum is compressed from 11.8 to 1.5 nm, obtaining a SCR of 7.87. The linear chirp induced by GVD in SMF1 is completely compensated near the pulse center (-1 ps $< T < 1$ ps). The second concatenation acquires a second stage SCR of 2.79 and a two-level SCR of 21.85, compressing the output spectrum of HNLF1 from 1.5 to 0.54 nm, and the precise compensated chirp is distributed in the area of -2.5 ps $< T < 2.5$ ps. A further SCR of 2.57 is gained in the last cascading, leading to a total SCR of 56.2 for the three-stage CDF. The simulation results have proved the feasibility of subpicosecond pulse spectral compression in a carefully designed CDF. An SCR of 56.2, which is the highest to our knowledge, is obtained. Following the principle of complete chirp compensation, more stages of CDF (>3) can be designed to realize a higher spectral compression ratio.

4 Application in the 7-Bit All-Optical ADC System

The soliton self-frequency shift effect is usually employed as a critical quantization principle in the all-optical analog-to-digital conversion system, which has been carefully studied in Refs. 18–21. The amount of frequency shift increases in proportion to the peak power of the input pulse to realize the power-to-wavelength conversion. The quantization resolution, which is a key factor for the whole system, is defined as[20]
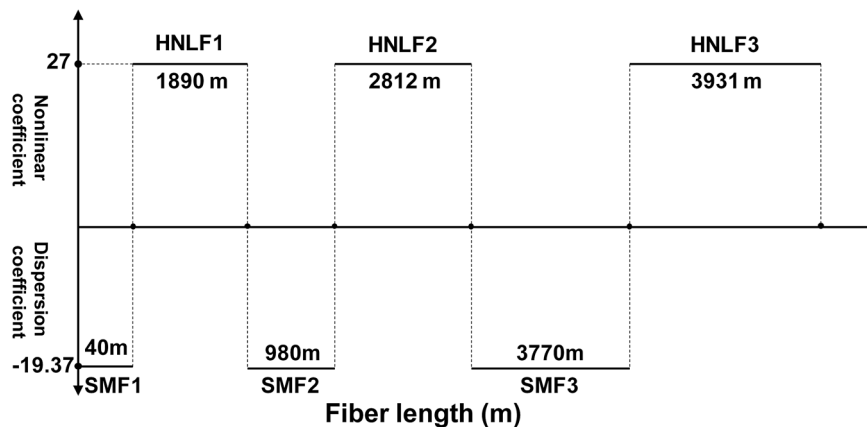

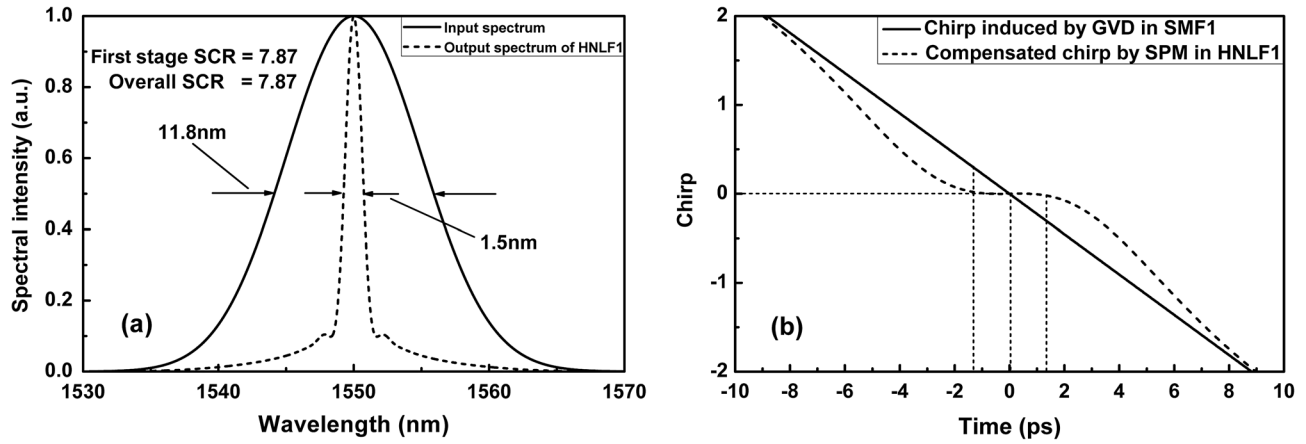**Fig. 4** Design of three-stage comb-like distributed fibers composed of SMF and HNLF.

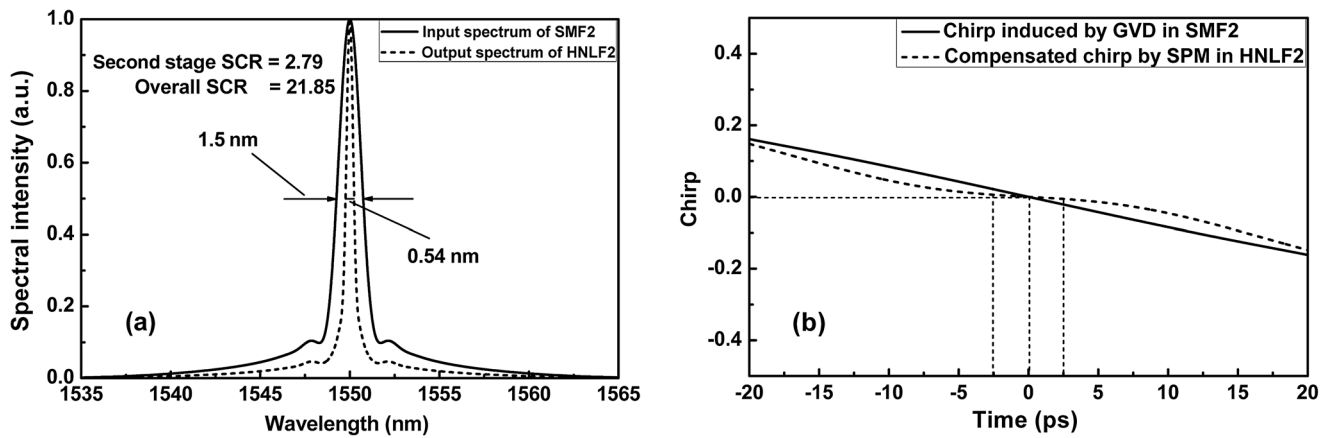**Fig. 5** (a) First stage spectral compression, (b) chirp compensation in the first concatenation.

Fig. 6 (a) Second stage spectral compression, (b) chirp compensation in the second concatenation.
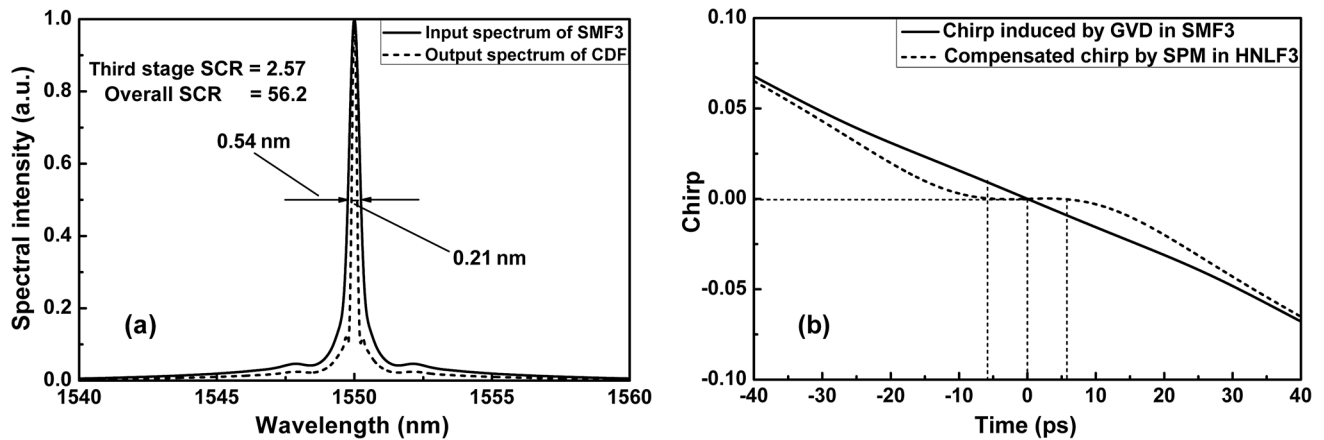

Fig. 7 (a) Third stage spectral compression, (b) chirp compensation in the third concatenation.

$$N = \log_2\left(\frac{\lambda_{\text{shift}} + \lambda_{\text{FWHM}}}{\lambda_{\text{FWHM}}}\right) = \log_2\left(1 + \frac{\lambda_{\text{shift}}}{\lambda_{\text{FWHM}}}\right), \qquad (16)$$

where λ_{shift} and λ_{FWHM} are the amount of the center wavelength shift and the spectral width of the pulse after Raman self-frequency shift, respectively. For a certain value of the input pulse's peak power, the amount of the center

wavelength shift (λ_{shift}) is a constant. Therefore, compressing the spectral width of the pulse after raman soliton frequency shifting (RSFS) is one feasible approach to increase the resolution of an all-optical ADC system. In this section, we propose and simulate a 7-bit all-optical analog-to-digital scheme based on Raman self-frequency shift and the wide-band wavelength-tunable spectral compression in CDF as shown in Fig. 8. In the simulation, a chirp-free
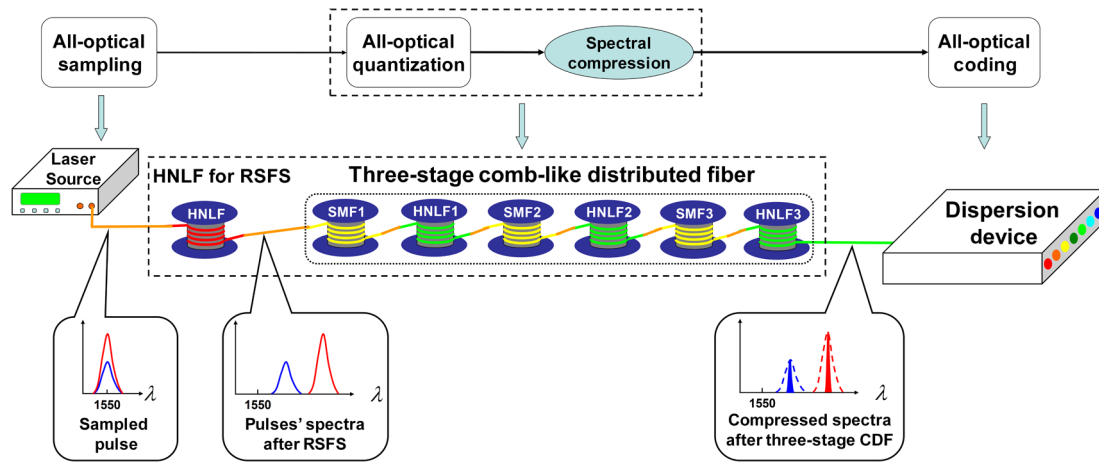
Fig. 8 Schematic diagram of all-optical ADC system based on RSFS and spectral compression in CDF.

Gaussian-shaped pulse, with a central wavelength of 1550 nm, a duration of 300 fs (FWHM), and 128 different peak powers from 25 to 30.969 W (with an interval of 0.047 W), is used as the all-optical sampled pulse and is injected into the HNLF for RSFS. The amount of RSFS is 31.8 nm which is from 1628.2 nm (25 W) to 1660 nm (31 W). A three-stage CDF is cascaded with the HNLF for RSFS to compress the spectra after RSFS. The parameters and lengths of SMF and HNLF employed in the CDF are shown in Tables 1 and 2, respectively. Figure 9 presents the simulated results of 128 output compressed spectra after propagating in the three-stage CDF. The maximum and minimum spectral compression ratios are 50.6 and 35.8, which

correspond to the minimum and maximum spectral widths of 0.17 and 0.23 nm after compression. The system resolution is determined by the maximum spectral width. Therefore, the 0.23-nm width is used in the Eq. (16) calculation and the calculated resolution of the all-optical quantization system is 7.1, which is the highest right now to the best of our knowledge.

It is easy to find from Fig. 9 that the spectral compression ratio is not a constant but keeps changing. The discussion should be made to explain why and how the spectral compression ratio changes in the wide-band wavelength-tunable spectral compression of CDF, and how it may affect the spectral compression quality.

As described above, the essential part of spectral compression in CDF is the balanced chirp compensation in each concatenation of SMF and HNLF. For the input pulse with different central wavelengths but with unchanged peak powers (i.e., Fig. 8), the balance would retain its stability and the GVD or SPM effect cannot break the tie, which leads to maintaining the spectral compression ratio as a constant. However, the pulses after RSFS not only have different central wavelengths but also have different peak powers. Different peak powers have little influence on the GVD effect, but sharply affect the SPM process,

Table 2 Second-order dispersion β_2, third-order dispersion β_3, the nonlinear coefficient γ, and the loss coefficient α of the single-mode fiber (SMF) and high nonlinearity fiber (HNLF).

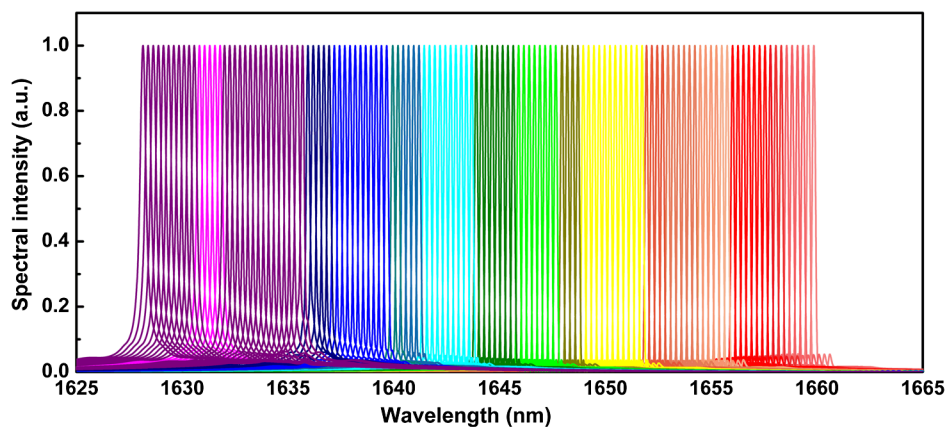|	First stage (m)	Second stage (m)	Third stage (m)
SMF	40	551	19216
HNLF	667.3	607	653

Fig. 9 Simulated results of the output spectrum after propagating in the three-stage CDF at 128 different input peak powers from 25 to 30.969 W (with an interval of 0.047 W).
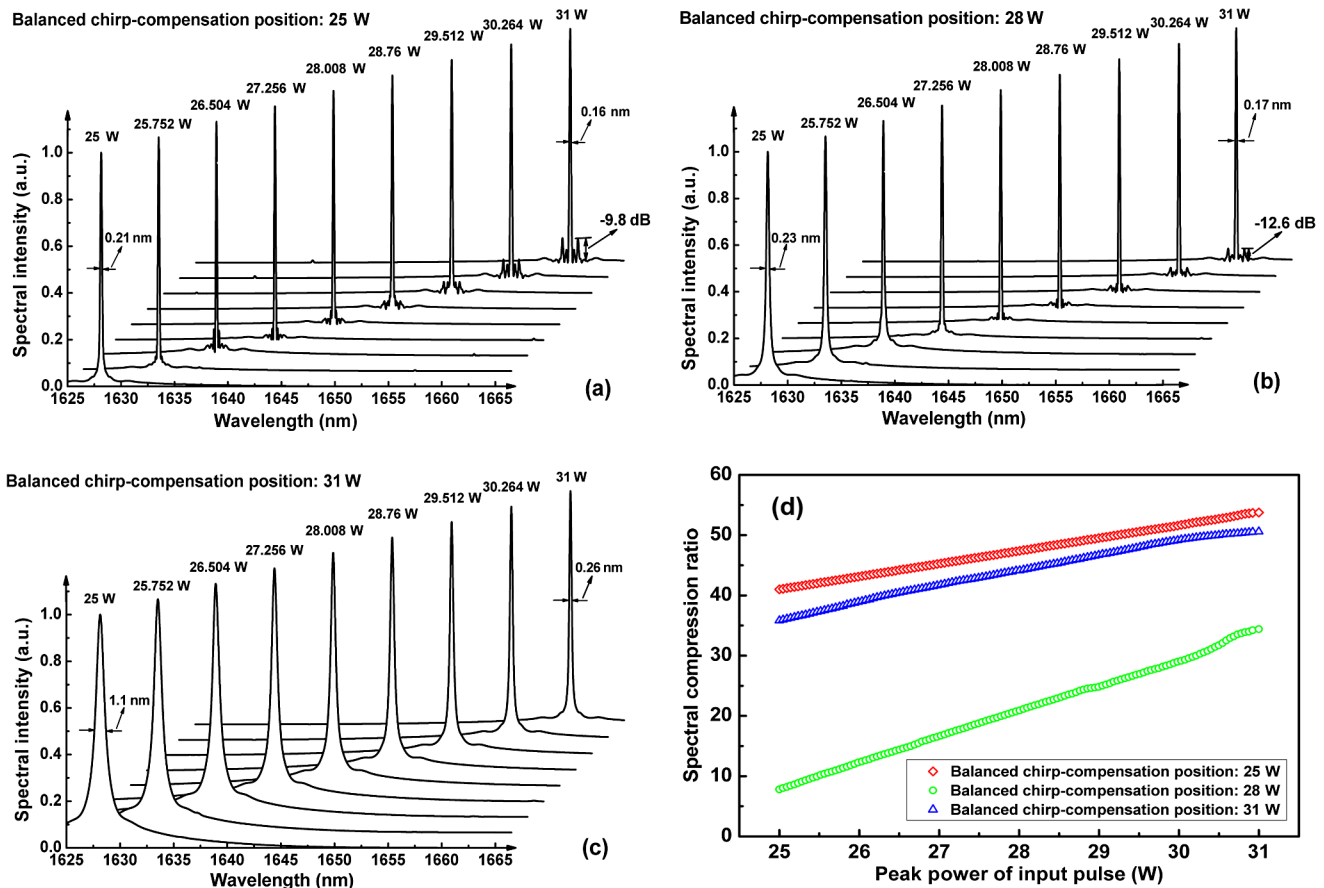
Fig. 10 Simulated spectral evolution under the condition of three different balanced chirp-compensation positions (a) the lowest peak power (25 W), (b) the middle peak power (28 W), (c) the highest peak power (31 W), (d) the spectral compression ratios change as a function of nine input peak powers under three different balanced chirp-compensation positions.

which may totally break the balance of chirp compensation. Here, we just assume that the chirp compensation is balanced for a pulse with a lower peak power, because as the peak power grows, the chirp induced by SPM would rapidly increase and make the chirp overcompensated and the spectral compression quality would be degraded [e.g., green line shown in the Figs. 2(a) and 2(b)]. Conversely, the balanced chirp compensation for a pulse with a higher peak power would result in insufficient chirp compensation and would decrease the spectral compression ratio for the pulses with lower a peak power [e.g., blue line shown in the Figs. 2(a) and 2(b)]. Therefore, it can be concluded that balanced chirp compensation for every spectrum in a wide-band wavelength-tunable range cannot be realized in the wide-band wavelength-tunable spectral compression of CDF. What we call in this paper the "position" of balanced chirp compensation (i.e., the value of the pulse's peak power when the chirp compensation is balanced) is the key to determining the spectral compression ratio and the spectral compression quality.

Taking the simulation shown in Fig. 9 as an example, we resimulate the spectral compression in a three-stage CDF 128 times under the condition of three different balanced chirp-compensation positions: the lowest peak power (25 W), the highest peak power (31 W), and the middle point (28 W). The simulation setups are same as those in Fig. 9 above.

The simulated results are shown in Fig. 10. Nine spectra (P = 25 W, 25.752 W, 26.504 W, 27.256 W, 28.008 W, 28.76 W, 29.512 W, 30.264 W, and 31 W) are sampled from the 128 times' simulation to clearly present the evolution of spectral compression under three conditions in Figs. 10(a)–10(c). Figure 10(d) exhibits the spectral compression ratios' change as a function of the input peak power.

The results just certify the analysis above. A higher spectral compression ratio can be obtained from 41 to 53.75 when the balanced chirp-compensation position is 25 W, leading to a maximum quantization resolution of 7.25-bit compared with the other two situations. However, simultaneously, spectral pedestal side-lobe components rapidly arise (−9.6 dB when 31 W) which may directly degrade the spectral compression quality and even disable the resolution improvement of the all-optical analog-to-digital conversion system.[22] On the other hand, although successfully avoiding the generation of spectral pedestal side-lobe components, the spectral compression ratio is too low to improve the quantization resolution when the balanced chirp-compensation position is 31 W. Therefore, as we can see, the middle position of the peak powers, which is 28 W here, just provides a trade-off between the spectral compression ratio and quality. A high enough quantization resolution and sufficient low spectral pedestal can be gained at the same
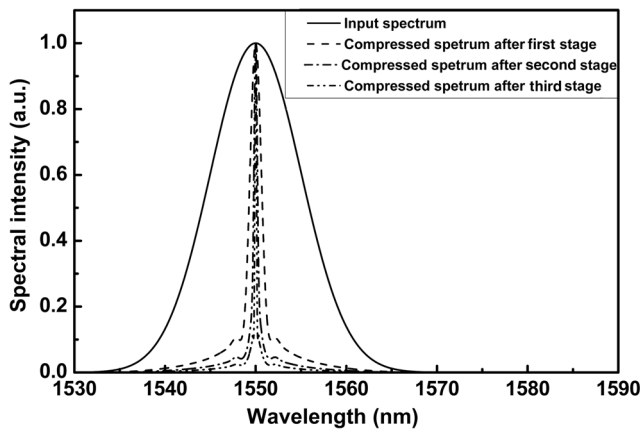
Fig. 11 Input spectrum and three-stage compressed spectra in the CDF simulation.

time. This feature is vital for the design of CDF applied in the all-optical analog-to-digital conversion system.

As shown in Fig. 11, which gathers three-stage compressed spectra from Figs. 5–7, it is clearer that the side-mode suppression ratio increases with the spectral compression. A qualitative discussion and explanation are given in this paper. The principle of spectral compression in the CDF is the complete chirp compensation around the pulse's center which had been presented above. In the first concatenation of SMF + HNLF, the spectrum is simultaneously compressed and the spectral side-lobe component is inevitably generated at the leading and trailing edges of the spectrum. The reason for the spectral side-lobe component generation is carefully analyzed in authors' previous papers.[22,23] Then, in the second stage, the central part of the spectrum continues to be compressed. However, it cannot be ignored that spectral side-lobe components at the leading and trailing edges are compressed at the same time. The spectral compression ratio is proportional to the peak power in some sense. Therefore, the central part of the spectrum with a higher peak power (corresponding to the central pulse) gains a bigger spectral compression ratio than that of the spectral side-lobe component, leading to an increase of the side-mode suppression ratio with the compression of the spectral width. This feature of spectral side-lobe component suppression in CDF is especially beneficial to the all-optical quantization resolution improvement proposed in this paper.

5 Conclusions

In summary, a three-stage CDF using a novel chirp-compensation method is proposed and numerically demonstrated. A strict mathematical derivation based on the complete nonlinear chirp-compensation principle is provided to calculate the fibers' lengths in CDF. Then, we design a three-stage CDF to verify low-pedestal wide-band wavelength-tunable spectral compression. The results show that a spectral compression ratio of 56.2 has been gained. The CDF's application in the 7-bit all-optical ADC system based on the soliton self-frequency shift is also introduced and simulated. The results show that the quantization resolution after spectral compression in CDF has been improved to 7.1-bit. Finally, we discuss how to select the balanced chirp-compensation position can make a compromise between the spectral compression ratio and spectral compression quality in the

CDF and draw the conclusion that the middle points of the input peak powers are the optimum choice.

References

1. S. V. Chernikov, R. Kashyap, and J. R. Taylor, "Comb-like dispersion-profiled fiber for soliton pulse train generation," *J. Opt. Lett.* **19**(8), 539–541 (1994).
2. J. Wang et al., "Pedestal-free 10-GHz pulse compression using comb-like dispersion profiled fibers and its application in 40-Gb/s OTDM systems," *J. Opt. Eng.* **42**(8), 2380–2383 (2003).
3. K. Igarashi et al., "Comb-like profiled fibre for efficient generation of high quality 160 GHz sub-picosecond soliton train," *J. Electron. Lett.* **41**(12), 688–690 (2005).
4. Y. Ozeki et al., "Repetition rate variable and wavelength-tunable picosecond optical pulse source employing square-wave-driven intensity modulator and comb-like profiled fiber," *J. IEEE Photon. Technol. Lett.* **17**(12), 2736–2738 (2005).
5. T. Inoue et al., "Optical pulse compression based on stationary rescaled pulse propagation in a comblike profiled fiber," *J. Lightwave Technol.* **24**(7), 2510–2522 (2006).
6. K. Igarashi et al., "Widely wavelength-tunable 40 GHz femtosecond pulse source based on compression of externally-modulated pulse using 1.4 km comb-like profiled fibre," *J. Electron. Lett.* **41**(14), 797–798 (2005).
7. Y. Ozeki et al., "Nearly exact optical beat-to-soliton train conversion based on comb-like profiled fiber emulating a polynomial dispersion decreasing profile," *J. IEEE Photon. Technol. Lett.* **17**(8), 1698–1700 (2005).
8. Y. Ozeki et al., "Generation of 1 THz repetition rate, 97 fs optical pulse train based on comb-like profiled fibre," *J. Electron. Lett.* **41**(19), 1048–1050 (2005).
9. T. Inoue et al., "Stationary rescaled pulse in dispersion-managed comblike profiled fiber for highly efficient and high-quality optical pulse compression," *J. Opt. Lett.* **32**(18), 2695–2697 (2007).
10. N. Nishizawa et al., "Wideband spectral compression of wavelength-tunable ultrashort soliton pulse using comb-profile fiber," *J. Opt. Express* **18**(11), 11700–11706 (2010).
11. K. Takahashi et al., "6 bit all-optical quantization using soliton self-frequency shift and multistage SPM-based spectral compression," in *Proc. Optoelectronics and Communications Conf. (OECC)*, p. 814, Academic, Kaohsiung, Taiwan, China (2011).
12. K. Takahashi et al., "Resolution upgrade toward 6-bit optical quantization using power-to-wavelength conversion for photonic analog-to-digital conversion," *J. Opt. Lett.* **38**(22), 4864–4867 (2013).
13. T. Satoh et al., "Power-saving approach toward 7-bit optical quantization for photonic analog-to-digital conversion," in *Proc. Lasers and Electro-Optics/Pacific Rim Conf.*, pp. 1–2 Academic, Kyoto, Japan (2013).
14. S. A. Planas et al., "Spectral narrowing in the propagation of chirped pulses in single-mode fibers," *Opt. Lett.* **18**(9), 699–701 (1993).
15. B. R. Washburn, J. A. Buck, and S. E. Ralph, "Transform-limited spectral compression due to self-phase modulation in fibers," *Opt. Lett.* **25**(7), 445–447 (2000).
16. E. R. Andresen, J. Thøgersen, and S. R. Keiding, "Spectral compression of femtosecond pulses in photonic crystal fibers," *Opt. Lett.* **30**(15), 2025–2027 (2005).
17. G. P. Agrawal, Ed., *Nonlinear Fiber Optics*, 4th ed., Academic Press, San Diego, California (2007).
18. T. Satoh et al., "10-GS/s 5-bit real-time optical quantization for photonic analog-to-digital conversion," *IEEE Photon. Technol. Lett.* **24**(10), 830–832 (2012).
19. K. Takahashi et al., "Resolution upgrade toward 6-bit optical quantization using power-to-wavelength conversion for photonic analog-to-digital conversion," *Opt. Lett.* **38**(22), 4864–4867 (2013).
20. T. Nishitani, T. Konishi, and K. Itoh, "Resolution improvement of all-optical analog-to-digital conversion employing self-frequency shift and self-phase-modulation-induced spectral compression," *IEEE J. Sel. Topics Quantum Electron.* **14**(3), 724–732 (2008).
21. Z. Y. Zhang et al., "Analog-to-digital converters using photonic technology," *Chin. Sci. Bull.* **59**(22), 2666–2671 (2014).

22. Y. Chen et al., "All-fiber low-pedestal spectral compression in a novel architecture based on an SMF cascading an HNLF-NOLM," *IEEE Photon. J.* **6**(5), 6100408 (2014).
23. Y. Chen et al., "All-fiber spectral compression and pedestal suppression in a two-stage structure employing a high nonlinear fiber interconnected with a high nonlinear fiber-nonlinear optical loop mirror," *Opt. Eng.* **53**(8), 086111 (2014).

Ying Chen is a full-time PhD student at the University of Electronic Science and Technology of China. He received his BS degree in electronic science and technology from ShangHai Jiaotong University and his MS degree in optical engineering from the College of Equipment in 2008 and 2010, respectively. His current research interests include all optical analog-to-digital conversion, nonlinear fiber optics, imaging sensors, and so on.

Zhiyao Zhang is an associate professor at the University of Electronic Science and Technology of China. He received his BS, MS, and DS degrees in optical engineering from the University of Electronic Science and Technology of China. His current research interests include all optical analog-to-digital conversion, nonlinear fiber optics, optical delay line, and so on.

Biographies of the other authors are not available.